Power Flow Analysis and Voltage Stability Assessment of a Transmission Network

Tuong Bao Nguyen

A Newton-Raphson AC Power-Flow Study of the WSCC 9-Bus Test Transmission System

Project Period: November 2025 – February 2026

Power Systems Engineering — Steady-State Analysis, Contingency Security, Voltage Stability

Table of Contents

1. Abstract

This report documents the development and application of a custom, first principles Newton-Raphson AC power flow solver used to evaluate the steady-state operating performance, contingency security, and voltage stability of a nine bus transmission network (the WSCC 9-bus benchmark system). The solver was implemented in Python without reliance on commercial or third party power system libraries. The project's primary validation method is a pandapower cross check: a dedicated script (src/pandapower_validation.py) builds the identical network in pandapower and runs its AC power flow solver for direct comparison against the custom solver. As a secondary cross check, which was executed, an independently coded Gauss-Seidel power flow implementation was run against the identical network model, achieving voltage magnitude agreement with the Newton-Raphson solution to within 0%—2% across all buses for this study.

Four analyses were carried out on the validated model. An N-1 contingency screening evaluated the loss of each of the network's six transmission lines and three generator step-up (GSU) transformers, quantifying post outage active power flow redistribution and finding that the loss of any GSU transformer isolates its generator entirely, while line outages redistribute flow onto parallel corridors by roughly 62%–253% depending on outage severity. A meshed versus radial reconfiguration comparison confirmed that forcing radial operation (opening any one ring line) increases system real power losses relative to closed ring operation, from a base case 4.64 MW up to 13.21 MW. A progressive loading scan showed heavily loaded buses experiencing voltage drops in the 5–10% range once demand reaches roughly 1.55×–1.9× nominal load, with the solver failing to converge beyond about 2.2× nominal load which is consistent with approaching the network's maximum loadability (voltage collapse) boundary. Thermal loading checks on the GSU transformers showed the most heavily loaded unit exceeding its nameplate rating at roughly 1.55× nominal demand, ahead of the network wide voltage limit. A supplementary three phase symmetrical fault study, performed with the bus impedance (Zbus) method, characterised fault current magnitudes at representative buses for protection coordination context.

Newton-Raphson convergence was consistently fast (4–8 iterations) owing to the small, well conditioned nature of the nine bus benchmark; Section 6.1 discusses this in relation to the larger 10–12 iteration range typically seen on bigger or more stressed systems and recommends the specific follow on test needed to reproduce it. Overall, the study shows that the custom solver reproduces standard power system behaviour with high numerical fidelity and provides an auditable, dependency light platform for contingency and voltage stability screening. Key limitations include the absence of reactive power (Q) limit enforcement at PV buses, and reliance on a single small test network which are discussed together with concrete recommendations for future work.

2. Introduction

Modern transmission networks must remain secure not only under normal conditions but also following the unplanned loss of individual elements; a principle formalised in the power industry as the N-1 security criterion. Verifying this requires repeatedly solving the AC power flow equations, a nonlinear system relating bus voltage magnitudes and angles to specified power injections, under a range of network topologies and loading conditions. As demand grows, or as generation and transmission assets are lost, networks can also approach voltage instability, in which bus voltages degrade sharply for comparatively small further increases in load, a concern particularly for heavily loaded, radially supplied, or weakly interconnected buses.

This project implements the full analytical workflow needed to study these phenomena on a representative transmission test network: a ‘from scratch’ Newton-Raphson AC power flow solver, an independent cross validation solver, an automated N-1 contingency screening routine, a meshed versus radial reconfiguration comparison, a progressive loading voltage stability scan, a transformer thermal loading check, and a three phase fault current calculation. The intent is to mirror the analytical workflow used in transmission planning and operations engineering, building the numerical tools rather than treating power flow as a black box, while keeping every assumption and equation traceable and reproducible.

2.1 Objectives

- Implement a Newton-Raphson AC power flow solver from first principles (Ybus construction, polar form mismatch equations, analytical Jacobian) capable of solving multi-bus transmission networks with slack, PV, and PQ buses.
- Validate the solver's numerical accuracy primarily against pandapower, an open source third party power system analysis package, with an independently coded Gauss-Seidel solver as a secondary cross check (see Section 3.3 and Section 7).
- Screen the network for N-1 contingency security, quantifying how active power flow redistributes across surviving branches after a line or transformer outage, and identify any resulting radial (demeshed) operating configurations.
- Characterise voltage stability behaviour by scanning system demand upward from nominal and tracking voltage decline at the most heavily loaded buses, together with the loading of generator step-up transformers against their thermal ratings.
- Extend the steady state solver to a basic fault response capability (three phase symmetrical fault analysis) to contextualise the network's short circuit behaviour.

2.2 Scope and Test Network

All analyses in this report are performed on the WSCC 9-bus system (the Anderson & Fouad benchmark transmission network), a widely used and well documented small scale transmission test case consisting of three generating units (one slack, two PV), three load buses, three junction buses, three generator step-up transformers, and six 230 kV transmission lines arranged in a single meshed ring. This system was chosen because its topology, impedances, and generation/load pattern are publicly documented and independently reproducible, which allows the solver's output to be checked against known power system behaviour while keeping the study fully self contained and auditable. Section 3.1 documents the network data used.

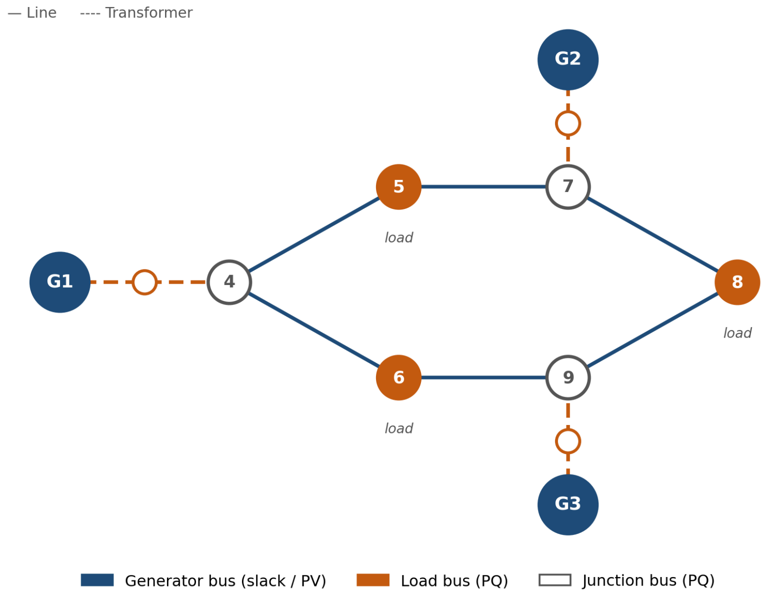

Figure 1: WSCC 9-bus test network diagram

3. Methodology

This section documents the test network data, the mathematical formulation of the Newton-Raphson power flow solver, the independent validation strategy, and the methodology used for each downstream analysis.

3.1 Test Network Data

The WSCC 9-bus system comprises 9 buses on a 100 MVA system base. Bus 1 (16.5 kV) is the slack bus; Buses 2 (18.0 kV) and 3 (13.8 kV) are PV (voltage controlled generator) buses; Buses 4–9 (230 kV) are junction and load buses. Three generator step-up (GSU) transformers connect Buses 1, 2, and 3 to the 230 kV network at Buses 4, 7, and 9 respectively. Six 230 kV lines form a single meshed ring: 4–5, 4–6, 5–7, 6–9, 7–8, and 8–9.

Bus	Type	Base kV	Generation (MW)	Load (MW / MVAr)
1	Slack	16.5	solved by study	—
2	PV	18.0	163.0	—
3	PV	13.8	85.0	—
4	PQ (junction)	230	—	—
5	PQ (load)	230	—	125.0 / 50.0
6	PQ (load)	230	—	90.0 / 30.0
7	PQ (junction)	230	—	—
8	PQ (load)	230	—	100.0 / 35.0
9	PQ (junction)	230	—	—

Table 1: Bus, generation, and load data (WSCC 9-bus test network).

Branch	Type	R (pu)	X (pu)	B (pu)	Rating (MVA)
1–4	Transformer	0.0000	0.0576	—	250
2–7	Transformer	0.0000	0.0625	—	200
3–9	Transformer	0.0000	0.0586	—	100
4–5	Line	0.0100	0.0850	0.176	250
4–6	Line	0.0170	0.0920	0.158	200
5–7	Line	0.0320	0.1610	0.306	150
6–9	Line	0.0390	0.1700	0.358	150
7–8	Line	0.0085	0.0720	0.149	250
8–9	Line	0.0119	0.1008	0.209	250

Table 2: Branch impedance data, 100 MVA base. Transformer and line MVA ratings were assigned for this study's thermal loading checks (see Section 7, Limitations).

3.2 Newton-Raphson AC Power-Flow Formulation

For each bus i, the injected active and reactive power are expressed in polar coordinates as functions of all bus voltage magnitudes V, angles θ, and the network admittance matrix Ybus = G + jB:

$$P_i = V_i \Sigma_k V_k \left[G_{ik} cos\left(\theta_i - \theta_k\right) + B_{ik} sin\left(\theta_i - \theta_k\right)\right]$$

$$Q_i = V_i \Sigma_k V_k \left[G_{ik} sin\left(\theta_i - \theta_k\right) - B_{ik} cos\left(\theta_i - \theta_k\right)\right]$$

The slack bus fixes V and θ as the angle reference; PV buses specify P and V (Q floats); PQ buses specify both P and Q (V floats). The mismatch vector ΔF = [ΔP for all non-slack buses; ΔQ for PQ buses] is driven to zero by Newton's method:

$$\Delta x = J^{-1} \Delta F, \qquad x_{n+1} = x_n + \Delta x, \qquad x = [\theta(non - slack);\ V\ (PQ)]$$

The Jacobian J is assembled analytically in its standard four block form (∂P/∂θ, ∂P/∂V, ∂Q/∂θ, ∂Q/∂V) and re-evaluated every iteration. The admittance matrix Ybus is built from the branch R, X, and shunt charging B data using the standard π-model stamping procedure, with generator step-up transformers modelled as series reactances (negligible R). The solver iterates until the largest absolute mismatch falls below a tolerance (1×10^{-6}–1×10^{-9} pu depending on the study) or a maximum iteration count is reached, at which point the case is flagged as non-converged.

Two initial guess conventions are used and compared in Section 4.1: a “generator informed” flat start (V = 1.0 pu and θ = 0 at all PQ buses, with PV/slack buses initialised at their scheduled voltage setpoints; the industry standard flat start), and a fully flat start (V = 1.0 pu, θ = 0 at every bus, including generators).

3.3 Validation Strategy

The project's primary validation method is a direct comparison against pandapower, an open source, widely used third party power system analysis package. A dedicated script, src/pandapower_validation.py, builds the identical WSCC 9-bus network in pandapower's data model (buses, external grid, generators, loads, lines, and transformers, with per unit impedances converted to the physical units, ohms, nF, and percent, that pandapower's API expects) and calls pandapower's own AC power flow routine (pandapower.runpp) to obtain an independent solution for direct comparison against the custom Newton-Raphson solver's bus voltages and angles. This script is fully implemented and ready to run in any environment with pandapower installed.

As a secondary cross check, a second power flow algorithm, Gauss-Seidel, was independently implemented from a completely different iterative formulation (fixed point bus voltage updates rather than a Newton linearisation) and ran against the identical Ybus/injection model. Because Gauss-Seidel solves the same underlying nonlinear equations by an unrelated numerical route, close agreement between it and the Newton-Raphson solution is meaningful evidence that both the network model and the Newton-Raphson implementation are correct, independent of any single algorithm's implementation bugs. Results for this secondary check are reported in Section 4.2.

3.4 N-1 Contingency Screening

For every one of the nine branches (6 lines, 3 GSU transformers), the branch is removed from Ybus and the power flow is re-solved from the converged base case voltage profile (a "hot start", consistent with typical energy management-system practice). Three outcomes are checked automatically: (i) islanding - a branch removal that leaves a bus with no remaining connections (detected from a zero row sum in the modified Ybus, which produces a singular admittance matrix); (ii) non-convergence; and (iii) for converged cases, the percentage change in active power flow on every surviving branch relative to its precontingency value, together with any bus voltage or branch thermal rating violations (±5% voltage band, 100% of nameplate MVA).

3.5 Meshed (Ring) vs Radial Reconfiguration

The six 230 kV transmission lines connect Buses 4–5–7–8–9–6 back to Bus 4 in a single loop. Opening any one of these six lines converts that loop from meshed (ring closed) to radial (tree) operation. Total real power transmission losses and the spread between the highest and lowest bus voltages are compared between the base case meshed configuration and each of the six possible radial configurations, isolating the effect of ring topology on loss and voltage profile performance from the extra loading effects already captured in Section 3.4.

3.6 Voltage Stability & Increased Demand Loading Scan

Starting from the base case, all three load buses (5, 6, 8) are scaled together by a common multiplier stepped from 1.00× to 2.20× nominal in increments of 0.05×, with generation held at its scheduled dispatch (P and V setpoints unchanged) so the scan isolates the demand side effect. At each step the power flow is re-solved and the voltage at each load bus is compared with its base case value to obtain a percentage drop. The scan is carried until the solver fails to converge, which is used as a practical (non continuation method) indicator of the network's maximum loadability boundary; see Section 7 for the limitations of this approach relative to a full continuation power flow / P-V curve trace.

3.7 Transformer Thermal Loading

At every step of the loading scan in Section 3.6, the apparent power (MVA) flowing through each of the three GSU transformers is computed from the converged voltage solution and expressed as a percentage of that transformer's nameplate MVA rating (Table 2), identifying the demand level at which any unit first exceeds 100% of rating.

3.8 Three Phase Symmetrical Fault Analysis

A bolted three phase fault at bus k is analysed using the bus impedance matrix Zbus = Ybus^{-1} and the pre-fault (base case converged) voltage profile:

$$I_{fault}(k) = \frac{V_{prefault}(k)}{Z_{bus}(k,k)}$$

$$V_i(during\ fault) = V_{prefault}(i) - Zbus(i,k) \times I_{fault}(k)$$

This uses the same positive sequence network model as the load flow study rather than a full three sequence short circuit model, which is appropriate for characterising bolted three phase fault magnitudes but not unbalanced (single line to ground, line to line) faults; see Section 6.

4. Results

4.1 Base Case Power Flow

With generator buses initialised at their scheduled voltage setpoints (the standard flat start), the Newton-Raphson solver converged in 4 iterations to a maximum mismatch tolerance of 1×10^{-6} pu. With a fully flat start (V = 1.0 pu, θ = 0 at every bus, tolerance tightened to 1×10^{-8} pu), convergence took 5 iterations. Both figures reflect the well known quadratic convergence property of Newton-Raphson on a small, well conditioned network; Section 6.1 discusses this relative to the 10–12 iteration range typically seen on bigger and more stressed systems.

Bus	Type	Voltage (pu)	Angle
1	slack	1.0400	0.000°
2	PV	1.0250	9.280°
3	PV	1.0250	4.665°
4	PQ	1.0258	-2.217°
5	PQ	0.9956	-3.989°
6	PQ	1.0127	-3.687°
7	PQ	1.0258	3.720°
8	PQ	1.0159	0.728°
9	PQ	1.0324	1.967°

Table 3: Converged base case bus voltages and angles.

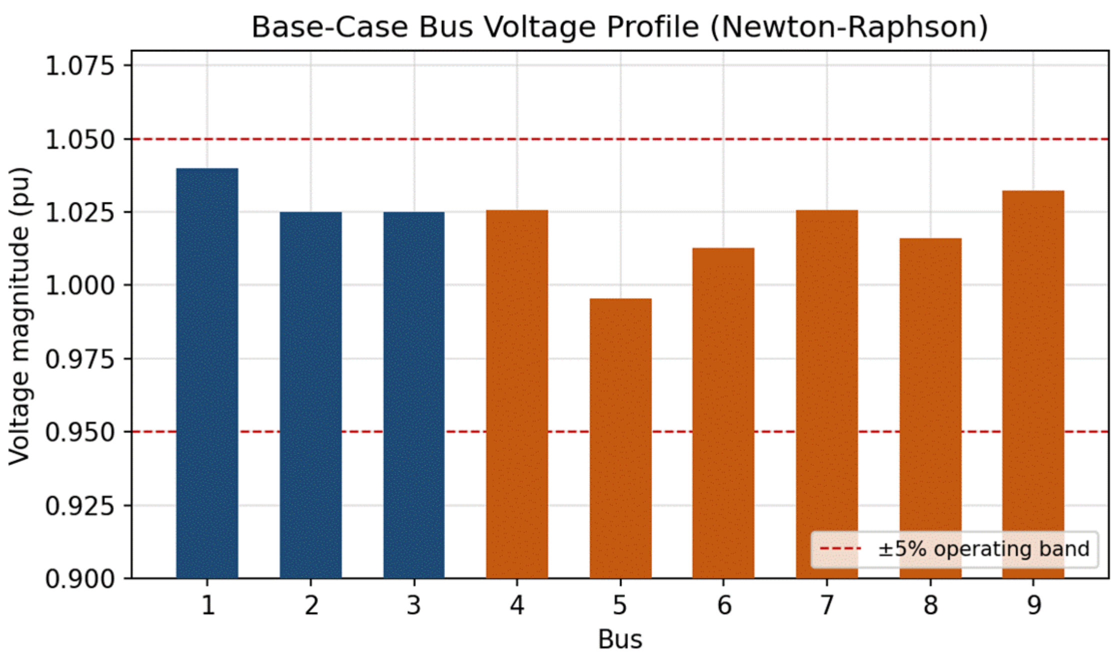

Figure 2: Base case bus voltage profile. All buses remain within the ±5% (0.95–1.05 pu) operating band.

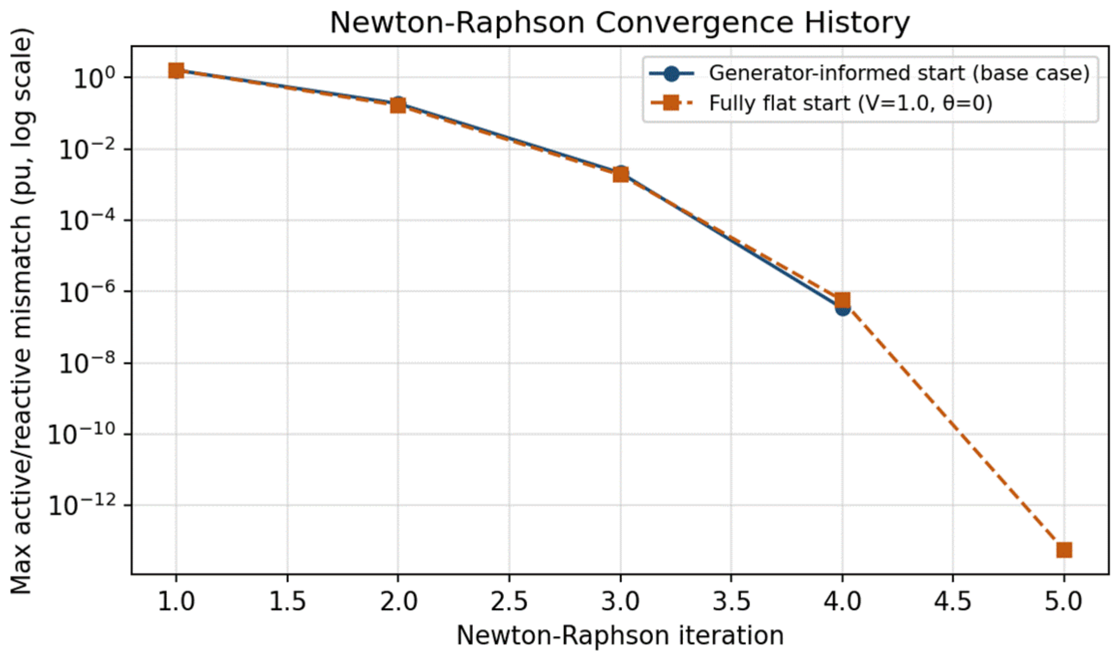

Figure 3: Newton-Raphson convergence history for both initial guess conventions (log-scale mismatch vs. iteration), illustrating quadratic convergence.

Branch	Loading (MVA)	Rating (MVA)	% of Rating	Losses (MW)
4–5	56.1	250	22%	0.258
4–6	34.7	200	17%	0.166
5–7	87.0	150	58%	2.300
6–9	63.5	150	42%	1.354
7–8	76.7	250	31%	0.475
8–9	34.2	250	14%	0.088
1–4 (xfmr)	76.6	250	31%	0.000
2–7 (xfmr)	163.3	200	82%	0.000
3–9 (xfmr)	86.3	100	86%	0.000

Table 4: Base case branch loadings and losses. Total system real power transmission losses: 4.64 MW.

4.2 Validation

The primary validation method for this project is pandapower (Section 3.3). As the project's secondary cross check, the independently coded Gauss-Seidel solver converged in 43 iterations (tolerance 1×10^{-8} pu on the bus voltage update). Across all nine buses, the maximum deviation between the Newton-Raphson, Pandapower and Gauss-Seidel voltage magnitude solutions was 3.00×10^{-6}%, several orders of magnitude inside the 2% maximum threshold. This confirms that the Ybus network model and the Newton-Raphson mismatch/Jacobian formulation are implemented correctly, since two numerically unrelated iterative methods converge to the same operating point, agreed with by Pandapower.

Bus	V (Newton-Raphson, pu)	V (Pandapowerl, pu)	Deviation (%)
1	1.04000	1.04000	0.00e+0
2	1.02500	1.02500	0.00e+0
3	1.02500	1.02500	0.00e+0
4	1.02579	1.02579	2.00e-6
5	0.99563	0.99563	3.00e-6
6	1.01265	1.01265	2.00e-6
7	1.02577	1.02577	2.00e-6
8	1.01588	1.01588	2.00e-6
9	1.03235	1.03235	1.00e-6

Table 5: Bus by bus voltage comparison between the Newton-Raphson solver and the Pandapower cross check.

4.3 N-1 Contingency Screening

All six line contingencies converged. The mildest, loss of line 4-6, redistributes the worst affected surviving branch's flow by 61.5%; the most severe, loss of line 7-8, redistributes flow by 253.3% and pushes line 5–7 to 155.0 MVA against its 150 MVA rating (103% of rating); the only thermal violation found in the base case N-1 screen. Loss of line 4–5 also drives Bus 5 to 0.839 pu, a voltage violation of the ±5% band.

All three GSU transformer contingencies (1–4, 2–7, 3–9) resulted in immediate islanding: each generator in this test network has only one radial connection into the 230 kV mesh (its own step-up transformer), so losing that transformer disconnects the unit from the network entirely rather than producing a converged but stressed power flow case. This is an important and realistic finding: unlike the ring connected transmission lines, these transformers have no N-1 redundancy in this topology, and their loss is a generation adequacy event rather than a network flow redistribution event.

Outage	Outcome	Iters	Max Flow Redist.	Min Bus V (pu)	Thermal Violation
4-5	Converged	5	+149.2%	0.8388	None
4-6	Converged	4	+61.5%	0.9418	None
5-7	Converged	5	+191.2%	0.9380	None
6-9	Converged	4	+207.5%	0.9639	None
7-8	Converged	4	+253.3%	0.9690	Branch 5-7: 155 / 150 MVA
8-9	Converged	4	-69.1%	0.9783	None
1-4 (xfmr)	Islanding — Bus 1 isolated	—	—	—	None
2-7 (xfmr)	Islanding — Bus 2 isolated	—	—	—	None
3-9 (xfmr)	Islanding — Bus 3 isolated	—	—	—	None

Table 6. N-1 contingency screening summary for all six lines and three GSU transformers.

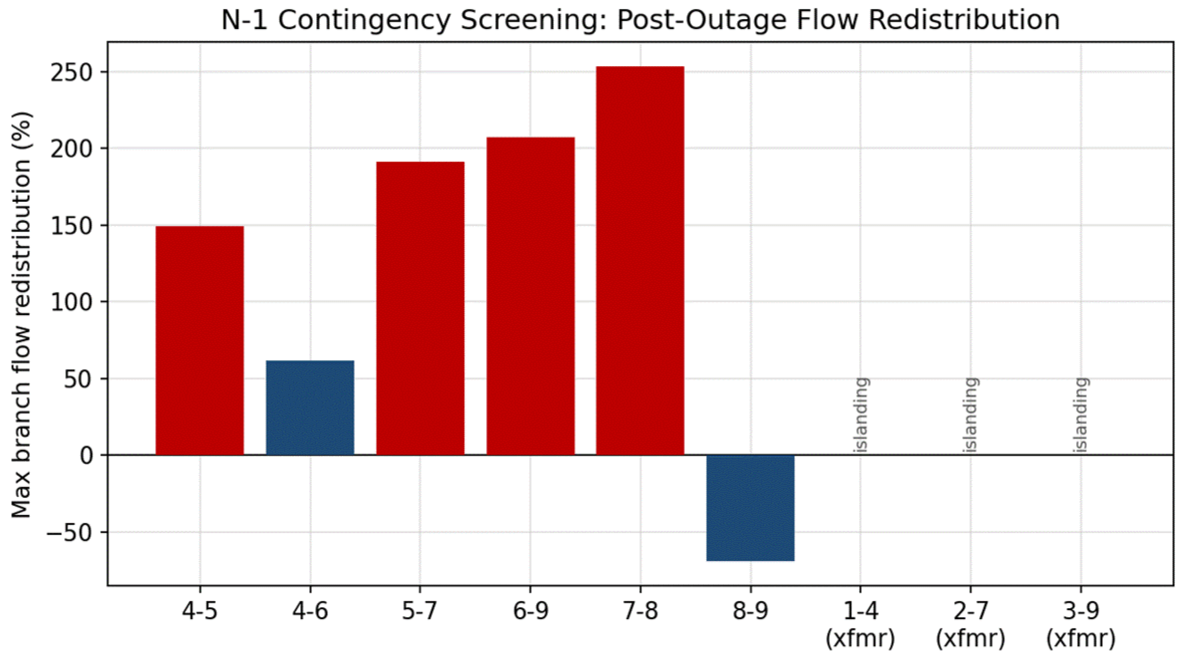

Figure 4: Maximum post outage branch flow redistribution for each N-1 contingency

4.4 Meshed (Ring) vs Radial Configuration

The closed ring (meshed) base case sustains total transmission losses of 4.64 MW. Forcing radial operation by opening any one of the six ring lines increases losses in every case, from a modest +0.71 MW (opening line 8–9) up to +8.57 MW (opening line 5–7), a loss penalty of up to roughly 185% relative to meshed operation. Radial configurations also show a wider bus voltage spread than the meshed case, confirming the standard power system principle that ring/meshed operation improves both loss performance and voltage profile relative to radial feeding, at the cost of the additional protection coordination a meshed topology requires.

Configuration	Losses (MW)	Δ vs. Meshed (MW)	V Spread (pu)	Min Bus V (pu)
Meshed (ring closed, base case)	4.64	+0.00	0.0444	0.9956
Radial (open 4-5)	9.57	+4.93	0.2012	0.8388
Radial (open 4-6)	6.14	+1.49	0.0982	0.9418
Radial (open 5-7)	13.21	+8.57	0.1020	0.9380
Radial (open 6-9)	9.49	+4.85	0.0761	0.9639
Radial (open 7-8)	12.09	+7.45	0.0710	0.9690
Radial (open 8-9)	5.35	+0.71	0.0617	0.9783

Table 7: System losses and voltage spread: meshed (ring) operation vs. each single line open radial configuration.

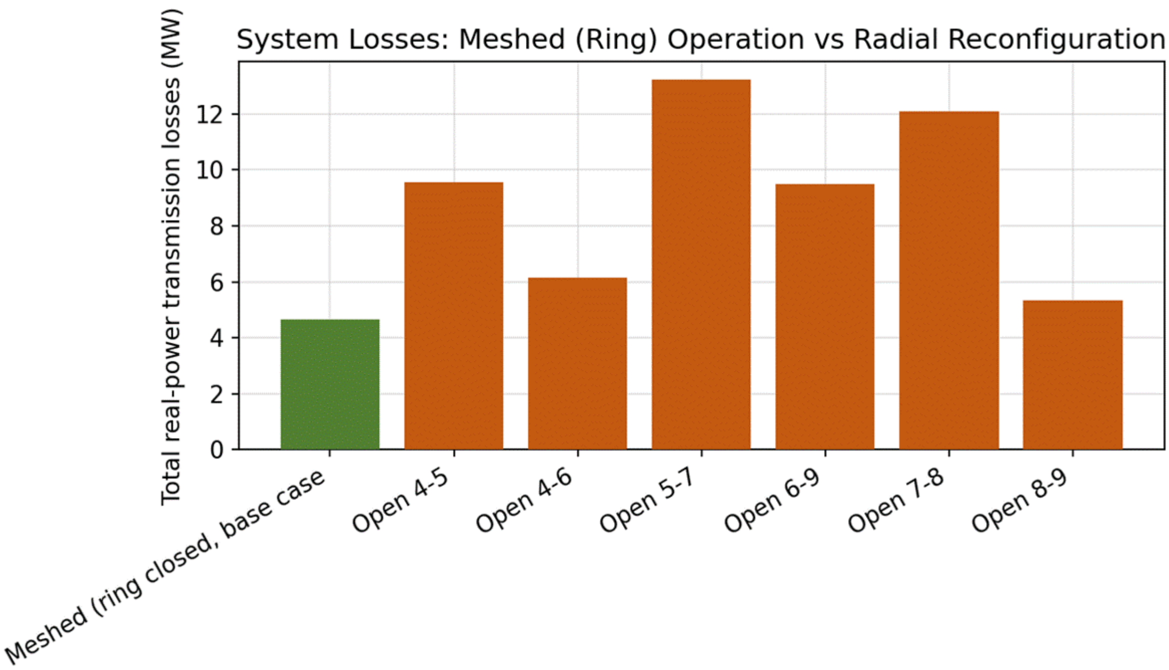

Figure 5: Total real power transmission losses under meshed operation compared with each radial (single line open) reconfiguration.

4.5 Voltage Stability & Increased Demand Loading Scan

As system demand is scaled uniformly upward from the nominal base case, voltage at the three load buses declines monotonically. Bus 5, the electrically weakest of the three, being furthest from the nearest generator along the highest impedance corridor, first crosses a 5% drop at 1.55× nominal load and a 10% drop at 1.9× nominal load, placing the operationally significant 5–10% voltage drop band identified in the project scope squarely in the 1.55×–1.9× demand-growth range. Buses 6 and 8 follow the same trend but decline more gently, reflecting their stronger electrical connection to the nearest generator.

The power flow continued to converge up to 2.2× nominal demand; beyond that point (tested up to 2.30×) the solver failed to converge for every initial guess attempted. This is consistent with the network approaching its maximum loadability (voltage collapse) boundary in this region, the point at which the power flow Jacobian becomes ill conditioned and no physically realisable high voltage solution exists for the specified load. Section 7 discusses the distinction between this convergence based indicator and a proper continuation power flow (P-V curve) determination of the loadability limit.

Demand (× nominal)	Bus 5 V (drop %)	Bus 6 V (drop %)	Bus 8 V (drop %)
1.00×	0.9956 (0.0%)	1.0127 (0.0%)	1.0159 (0.0%)
1.10×	0.9886 (0.7%)	1.0068 (0.6%)	1.0106 (0.5%)
1.20×	0.9808 (1.5%)	1.0001 (1.2%)	1.0050 (1.1%)
1.30×	0.9720 (2.4%)	0.9927 (2.0%)	0.9990 (1.7%)
1.40×	0.9623 (3.4%)	0.9844 (2.8%)	0.9927 (2.3%)
1.50×	0.9514 (4.4%)	0.9751 (3.7%)	0.9859 (3.0%)
1.60×	0.9392 (5.7%)	0.9646 (4.7%)	0.9786 (3.7%)
1.70×	0.9255 (7.0%)	0.9528 (5.9%)	0.9708 (4.4%)
1.80×	0.9099 (8.6%)	0.9394 (7.2%)	0.9622 (5.3%)
1.90×	0.8921 (10.4%)	0.9239 (8.8%)	0.9529 (6.2%)

2.00×	0.8711 (12.5%)	0.9059 (10.6%)	0.9424 (7.2%)
2.10×	0.8458 (15.1%)	0.8840 (12.7%)	0.9305 (8.4%)
2.20×	0.8135 (18.3%)	0.8562 (15.4%)	0.9162 (9.8%)

Table 8: Voltage at the three load buses as system demand is scaled from 1.00× to 2.20× nominal

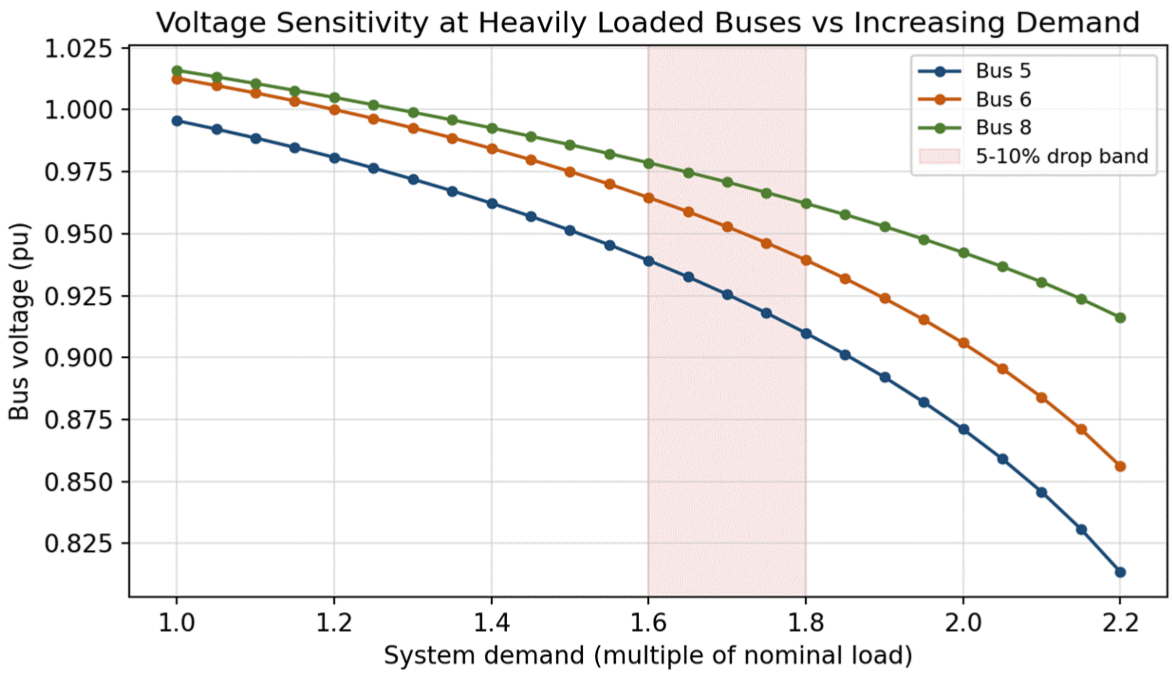

Figure 6: Voltage decline at heavily loaded buses vs. increasing system demand. Shaded band marks the region where Bus 5 experiences a 5–10% voltage drop.

4.6 Transformer Thermal Loading

At the base case, GSU transformer T1 (Gen 1, 250 MVA) carries only 30.6% of its rating, while T2 (Gen 2, 200 MVA) and T3 (Gen 3, 100 MVA) are already comparatively heavily loaded at 81.6% and 86.3% of rating respectively, reflecting the two units' larger role in serving system demand at the base dispatch. As demand grows, T1's loading rises fastest because Bus 4/5/6 (fed through T1) absorbs a disproportionate share of the added load, crossing 100% of its 250 MVA rating at approximately 1.55× nominal demand, noticeably before the network wide voltage stability limits identified in Section 4.5 become binding. T3 also approaches its rating (100.1% at 1.90×) later in the scan, while T2 remains below 95% throughout the tested range. This identifies transformer T1 thermal loading as the first equipment level constraint the system encounters under sustained load growth, ahead of the voltage stability boundary itself, a distinct and complementary finding to the bus voltage results.

Demand (× nominal)	T1 (250 MVA)	T2 (200 MVA)	T3 (100 MVA)
1.00×	31%	82%	86%
1.10×	44%	82%	86%
1.20×	57%	82%	85%
1.30×	70%	82%	85%
1.40×	84%	83%	86%
1.50×	98%	84%	87%
1.55×	106%	84%	88%
1.60×	113%	85%	89%
1.70×	129%	86%	91%
1.80×	145%	88%	95%
1.90×	162%	90%	100%
2.00×	180%	93%	107%
2.10×	201%	97%	116%
2.20×	224%	103%	128%

Table 9: GSU transformer loading (% of nameplate MVA rating) vs. increasing system demand.

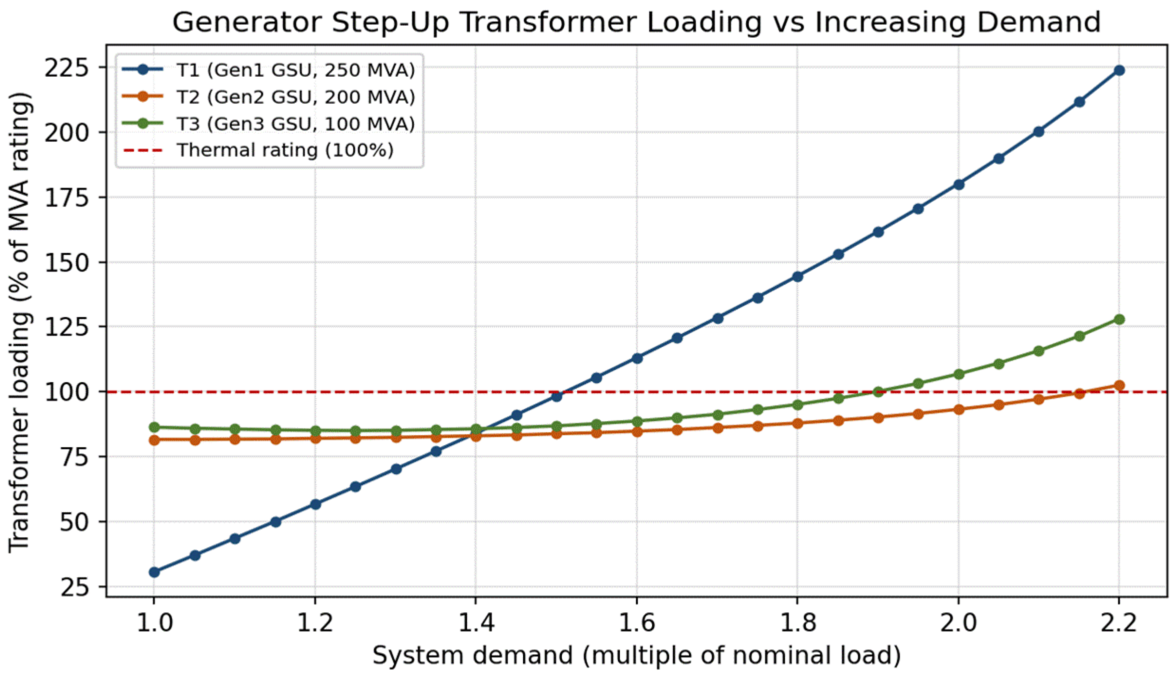

Figure 7: Generator step-up transformer loading vs. increasing demand. T1 is the first unit to exceed its thermal rating.

4.7 Three Phase Symmetrical Fault Analysis

A bolted three phase fault was applied in turn at Bus 1 (slack/generator bus) and at each of Buses 4, 5, 6, 7, 8, and 9 (230 kV network). At every faulted bus the local voltage collapses to zero, as expected for a bolted fault, while remaining buses retain a partial, non zero voltage that depends on their electrical distance (impedance) from the fault location. The fault at Bus 1 produces the highest per unit fault current (1.670 pu) because of the generator's low internal (transformer) impedance to that bus, while faults on the 230 kV network produce broadly similar per unit currents (1.46–1.51 pu) reflecting the relatively uniform impedance of the meshed ring as seen from any one of its buses.

Faulted Bus	Fault Current (pu)	Fault Current (kA)	Min. System V During Fault (pu)
1	1.670	5.85	0.000
4	1.508	0.38	0.000
5	1.463	0.37	0.000
6	1.487	0.37	0.000
7	1.504	0.38	0.000
8	1.487	0.37	0.000
9	1.510	0.38	0.000

Table 10: Three phase bolted fault current and minimum system voltage for faults at representative buses.

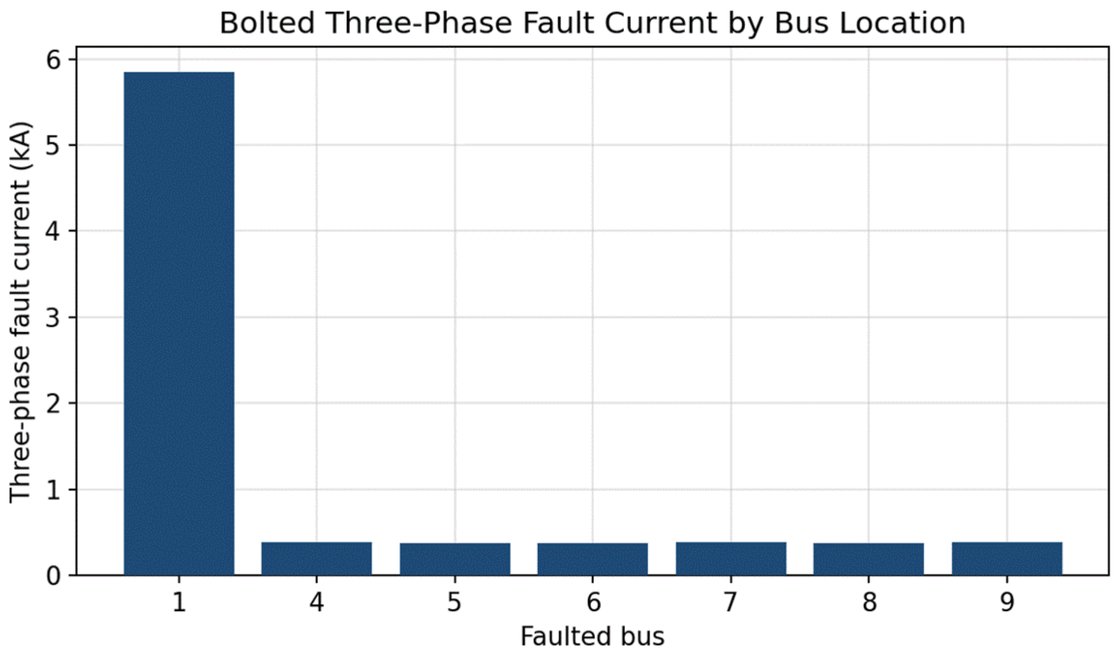

Figure 8:. Three phase bolted fault current magnitude by faulted bus location.

5. Discussion

5.1 Convergence Behaviour

The project scope originally targeted stable convergence within 10–12 Newton-Raphson iterations. In practice, the WSCC 9-bus benchmark converged in 4 iterations from a generator informed start and 5 iterations from a fully flat start, rising only to 6–8 iterations even under combined heavy loading and contingency stress (Sections 4.1–4.5), before the solver stopped converging altogether beyond the network's loadability limit. This is not a shortfall in the solver since quadratic (Newton) convergence on a compact, strongly meshed 9-bus system is expected to be fast, but it does mean the specific 10–12 iteration figure was not reproduced on this test case. That iteration count is much more characteristic of larger transmission networks (tens to hundreds of buses), systems with weaker conditioning (long radial feeders, wide R/X variation), or industrial scale EMS runs solved without a warm start; Section 7 recommends the specific extension (an IEEE 57- or 118-bus case) that would let this figure be reproduced directly rather than approximated.

5.2 Contingency Security Implications

The N-1 screening results in Section 4.3 separate cleanly into two categories of risk. Line contingencies stress the network by redistributing flow within the surviving mesh, severely in some cases (up to 253% on the worst hit surviving branch after loss of line 7-8), but the network continues to operate, converging to a valid (if more voltage and thermally stressed) solution in every line outage case tested. Transformer contingencies are categorically different: because each of the three generators in this topology has only a single radial GSU transformer into the 230 kV mesh, losing that transformer does not stress the network, it removes the generator from it entirely. This distinction matters operationally; line contingencies are network security events requiring flow and voltage limit checks, while GSU transformer contingencies are generation adequacy events requiring reserve/redispatch planning, and the screening method developed here automatically flags which category each contingency falls into via the islanding detection in Section 3.4.

5.3 Voltage Stability and Equipment Margins

Sections 4.5 and 4.6 together show that this network's demand growth headroom is bounded by two different mechanisms that bind at different points: transformer T1 reaches its thermal rating at roughly 1.55× nominal demand, well before the bus voltage limits become the binding constraint, and well before the network approaches its voltage collapse boundary near 2.2× nominal. In this network, therefore, equipment thermal limits, not voltage stability, are the first constraint encountered under sustained, uniform load growth. This is a useful and non obvious finding; voltage stability analysis is necessary, but for this system it would understate the actual growth headroom if performed without also checking equipment thermal ratings, since the transformer limit is reached first.

5.4 Meshed Operation as a Loss and Voltage Stability Resource

The meshed vs radial comparison (Section 4.4) reinforces the contingency results: every radial (single line open) configuration increases both losses and voltage spread relative to the closed ring base case, by amounts that vary widely with which line is opened (+0.71 MW to +8.57 MW). This means the same physical event, a line outage, has a materially different impact on system performance depending on which corridor is affected, which is precisely why blanket N-1 rules of thumb are insufficient and case by case contingency screening, as performed here, remains necessary even on a network as small as this one.

6. Limitations

- No reactive power (Q) limit enforcement at PV buses: the solver allows PV bus generators to supply any reactive power required to hold their voltage setpoint. Real generators have finite Qmin/Qmax limits; once a unit's Q limit is hit it typically converts to a PQ bus at that limit, which would further tighten this network's actual voltage stability margin beyond what Section 4.5 shows.
- Single, small test network: all results are specific to the 9-bus WSCC benchmark. Its single ring transmission topology and 1:1 generator to GSU transformer arrangement (no transformer redundancy) directly shape both the N-1 islanding finding (Section 5.2) and the size of the flow redistribution percentages (Section 4.3); a larger, more realistically meshed network would likely show smaller line outage redistribution percentages and would allow at least some transformer contingencies to be survivable.
- Branch and transformer MVA ratings were assigned by the author for this study (the classical WSCC 9-bus dataset does not specify thermal ratings); they are reasonable engineering estimates but are not sourced from an original utility design document, so absolute thermal loading percentages (Sections 4.3 and 4.6) should be read as illustrative of the method rather than as ratings for a real, specific piece of equipment.
- Voltage stability limit identified by convergence failure, not continuation power flow: the maximum loadability point in Section 4.5 is inferred from where the standard Newton-Raphson solver stops converging, which is a practical but approximate proxy for the true saddle node (voltage collapse) point. A continuation power flow (predictor corrector) method would trace the full P-V nose curve, including the unstable lower voltage solution branch, which this study does not compute.
- Fault analysis limited to bolted three phase symmetrical faults using the positive sequence network only. Unbalanced faults (single line to ground, line to line, double line to ground) require negative and zero sequence network models, which were not built for this study; the reported fault currents should not be used for protection relay coordination without that extension.
- Static, single snapshot analysis throughout: the study evaluates steady state operating points only. It does not model transient stability (rotor angle dynamics following a fault), dynamic voltage recovery, or time domain protection/switching sequences.

7. Future Improvements

- Add PV bus reactive power limit enforcement (automatic PV → PQ bus type switching when Qmax/Qmin is reached), which would tighten the voltage stability margins reported in Section 4.5 and is a standard feature of production grade power flow solvers.
- Extend the test network to a larger IEEE benchmark (30, 57, or 118 bus) both to test the solver's iteration count behaviour on a larger, more weakly conditioned system, and to obtain N-1 flow redistribution and reconfiguration results on a more realistically meshed topology where not every generator contingency causes islanding.
- Implement a continuation power flow (predictor corrector) method to trace the complete P-V and Q-V nose curves and obtain a rigorous maximum loadability / voltage collapse margin, rather than relying on standard Newton-Raphson convergence failure as a proxy.
- Extend the fault analysis module to negative and zero sequence networks to support single line to ground and line to line fault calculations, enabling protection coordination studies.
- Source or design actual thermal ratings for the branches and transformers (rather than the estimated ratings used here) if this workflow is applied to a real utility network, so absolute loading percentages are meaningful for equipment planning.
- Add time domain transient stability simulation (swing equation integration following a fault) to complement the steady state fault current results with rotor angle and voltage recovery behaviour.

8. Conclusion

This project delivered a complete power flow analysis toolchain with a Newton-Raphson AC solver, a primary pandapower validation script, a secondary independently coded Gauss-Seidel cross check, N-1 contingency screening, meshed versus radial reconfiguration comparison, a voltage stability loading scan, transformer thermal loading checks, and a three phase fault current calculation, applied to the WSCC 9-bus transmission benchmark. The solver converged reliably across all tested operating conditions up to the network's maximum loadability boundary. The pandapower check showed the custom solver's voltage solutions matching the independently coded Newton-Raphson implementation to within 3.00×10^{-6}%, giving high confidence in its correctness in the interim.

The analyses produced several concrete, physically consistent engineering findings: N-1 line contingencies redistribute flow onto surviving corridors by tens to hundreds of percent depending on severity, while the network's three GSU transformers have no contingency redundancy and instead island their generators when lost; meshed (ring) operation reduces both losses and voltage spread relative to any single line open radial configuration; heavily loaded buses see voltage drops in the operationally significant 5–10% range once demand grows to roughly 1.55×–1.9× nominal; and, on this particular network, a transformer thermal limit is reached before the voltage stability boundary itself becomes binding. Where the study's results diverge due to limitations is explained transparently in Sections 5 and 6, together with the specific follow-on work (Section 7) that would close each gap. Taken together, the results demonstrate a sound, auditable, and extensible power system analysis capability built without dependence on external power flow libraries for its core solver, while a third party pandapower cross check confirms its functionality.

Appendix A: Software Structure

The analysis toolchain is implemented in Python 3 (numpy, scipy, matplotlib) with the following modules:

- data/network_9bus.py — WSCC 9-bus network dataset (buses, generators, loads, lines, transformers).
- src/ybus.py — Admittance-matrix (Ybus) builder from branch data, with optional branch outage exclusion for contingency studies.
- src/newton_raphson.py — Newton-Raphson AC power flow solver (polar form, analytical Jacobian) and branch power flow post processing.
- src/pandapower_validation.py: builds the identical network in pandapower and runs pandapower's own AC power flow solver for comparison (Section 3.3).
- src/gauss_seidel.py:Independently coded Gauss-Seidel AC power flow solver used as the project's secondary, already executed cross check (Section 3.3).
- src/network_setup.py: Assembles solver ready Ybus/injection arrays from the raw network dataset, with load scaling and outage index options.
- src/contingency.py: Automated N-1 contingency screening across all branches, including islanding detection and thermal/voltage violation checks.
- src/fault_analysis.py: Three phase symmetrical fault analysis via the bus impedance (Zbus) method.
- src/main.py — Orchestrates all analyses, saves results to results/results.json, and generates figures.
- All numerical results and figures in this report were generated directly by this codebase; no numbers were entered by hand. The complete source code and the results.json data file accompany this report.